SHOCK WAVE STUDIES OF THE PHYSICAL PROPERTIES OF GASES

R. I. SOLOUKHIN

Usp. Fiz. Nauk **68**, 513-528 (July, 1959)

INTRODUCTION

THE use of shock-wave methods in laboratory investigations of the physical and physico-chemical properties of various gases at high temperatures is constantly increasing. High gas temperatures and pressures can be produced by such means and the gasdynamical scheme of the process involved is fairly simple. The effects of physico-chemical transformations of the medium can thus be taken into account, furnishing interesting information concerning nonequilibrium thermodynamic processes induced by the heating of a gas in a shock wave.

Shock waves can be used to study not only the thermodynamic equilibrium states of a gas but also the course of the establishment of equilibrium, i.e., to investigate the kinetics of such non-equilibrium processes as dissociation, high-temperature oxidation, relaxation processes of energy exchange between internal degrees of freedom of molecules and between electrons and positive ions.

For the purpose of obtaining the most exact information concerning gaseous states during short time intervals ($10^{-6} - 10^{-4}$ sec) new pulse techniques are being developed for measuring temperature, density, pressure, degree of ionization, emissivity, absorptivity, electrical conductivity and other gas parameters by modern physical measuring methods.

In the present article we shall consider only a few of the numerous investigations of shock waves in gases, limiting ourselves to the establishment of thermodynamic equilibrium behind shock fronts in various gases and touching on some of the most interesting methodological work.

For the properties of strong shock waves and the internal structure of shock fronts with emission and radiative heat exchange taken into account we refer the reader to the extensive review by Zel'dovich and Raĭzer,[1] who have written many original papers on strong shock waves.

1. SELECTION OF A METHOD OF PRODUCING AND UTILIZING SHOCK WAVES

The variation of the gas parameters behind a shock front depends on the gas dynamics of the process involved, i.e., the type and form of shock wave (one-dimensional density jump, detonation wave, shock wave generated by a rapidly moving body etc.) as well as on its strength and the physico-chemical properties of the medium in which the wave is propagating. Unambiguous recording of the physico-chemical transformations requires exact determination of the process in the absence of such transformations. We shall therefore not analyze various methods involving techniques for focusing shock waves as well as such two-dimensional cases as the shock wave at the nose of a projectile, and shall confine ourselves to methods that produce a sufficiently extended and homogeneous region of gas with known parameters behind the shock front. Most suitable for this purpose are shock tubes and plates driven by the detonation of explosives.

Upon rupture of a diaphragm separating two gases at different pressures in a long duct of constant cross section, a shock wave propagates at constant velocity in the direction of the lower-pressure gas.[2] The strength of this shock wave depends principally on the initial pressure difference at the diaphragm and on the ratio of the sound velocities in the two gases; for the production of a high temperature behind the shock wave the velocity of sound must be great in the higher-pressure gas and small in the investigated lower-pressure gas.

The schlieren photograph frames in Fig. 1 show the propagation of a shock wave in an inert gas within a shock tube of square cross section at about two meters from the location of the ruptured

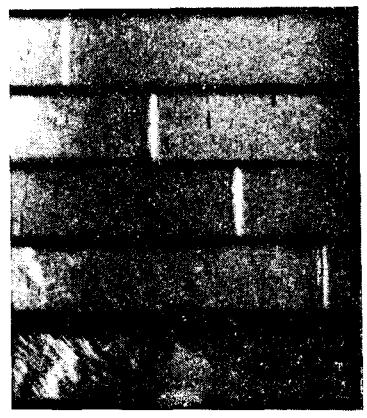

FIG. 1. Shock wave propagation in carbon dioxide. M ~ 6. 40,000 frames per second.

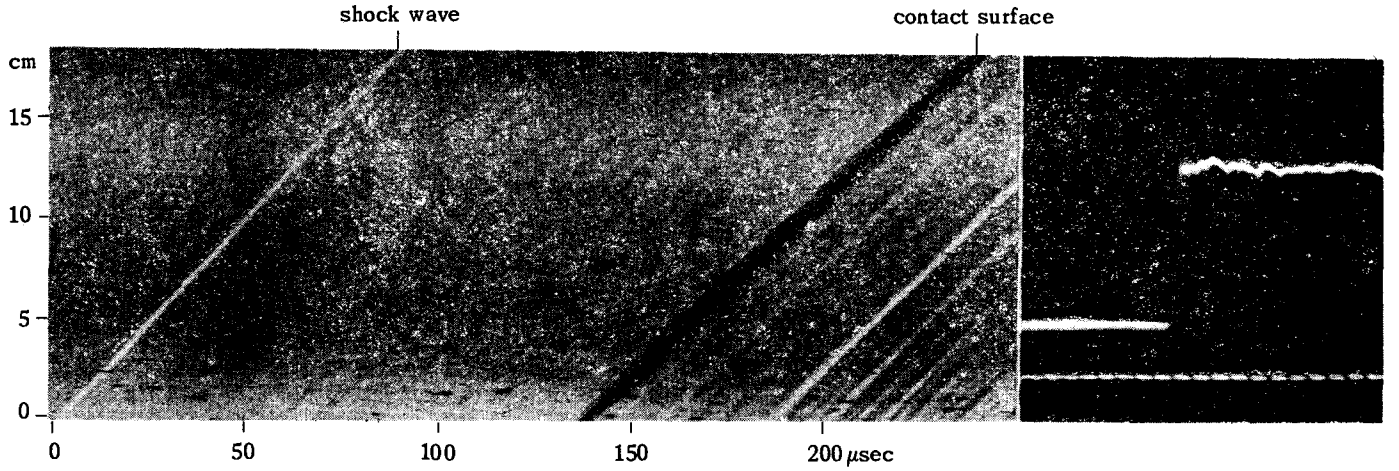

FIG. 2. Moving-film photograph of shock wave motion and oscillogram of pressure behind shock front. 10 μsec time markings.

diaphragm.[3] A homogeneous gas region heated by the shock wave is behind the plane shock front. The extent of this region is determined mainly by the strength of the shock and the distance traversed by the wave starting from the diaphragm. The rear boundary of this hot gas region is the contact surface separating the heated gas from the cold gas flowing out of the high-pressure section. The homogeneity of the gas flow behind the shock wave can be judged, for example, from the moving-film photograph in Fig. 1 and from the oscillogram of pressure behind the shock front recorded by a piezoelectric pulse gauge[4] (Fig. 2). The velocity of the shock wave is determined from the slope of the first disturbance; the lines of smallest slope, which are the traces of optical inhomogeneities that do not move with respect to gas particles, and the trace of the contact surface also provide an independent determination of the gas flow velocity behind the shock wave.

The practical upper limit of temperature behind a shock front which can be produced in a shock tube may be about 20,000° K.

The shock-tube method suffers from a number of shortcomings and limitations resulting mainly from the presence of walls. The gas layer forming at the wall behind the shock wave disturbs the one-dimensional flow pattern. The influence of the boundary layer is shown especially clearly in the propagation of a shock wave reflected from a flat wall and moving against the flow produced by the incident wave.[6] The resulting complex picture, which is shown in Fig. 3 for a shock wave in argon, essentially limits the use of reflected shock waves, which can otherwise be useful because of the fact that the gas behind the reflected wave is at rest with respect to the tube wall.[7] The study of luminosity and the degree of ionization behind a shock wave is influenced by this wall effect through the generation of easily excited impurities that strongly influence the course of the process and the accuracy of measurement.

The use of explosive charges is less convenient than the shock-tube method from the point of view of accessibility and recording techniques.[8] However, the former removes the wall-effect limitation and can produce shock waves with velocities higher than 8 km/sec in gases initially at atmospheric pressure. The strength of the shock wave is determined by using metal plates of different thicknesses between the surface of the explosive charge and the gas. Both the velocity U of the shock wave generated in the gas and the velocity u of the flow behind it, which is determined from the velocity of the metal plate, are constant over a considerable portion of the wave path. Independent measurements of these quantities make it possible to determine the pressure and density ratios for the shock wave from the following simple relations:

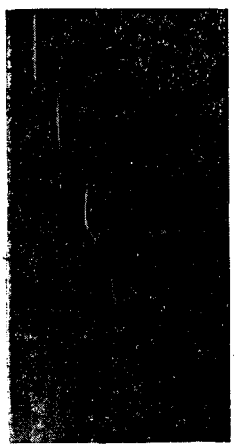

FIG. 3. Schlieren photograph of shock wave reflection in argon from the end of a closed tube.

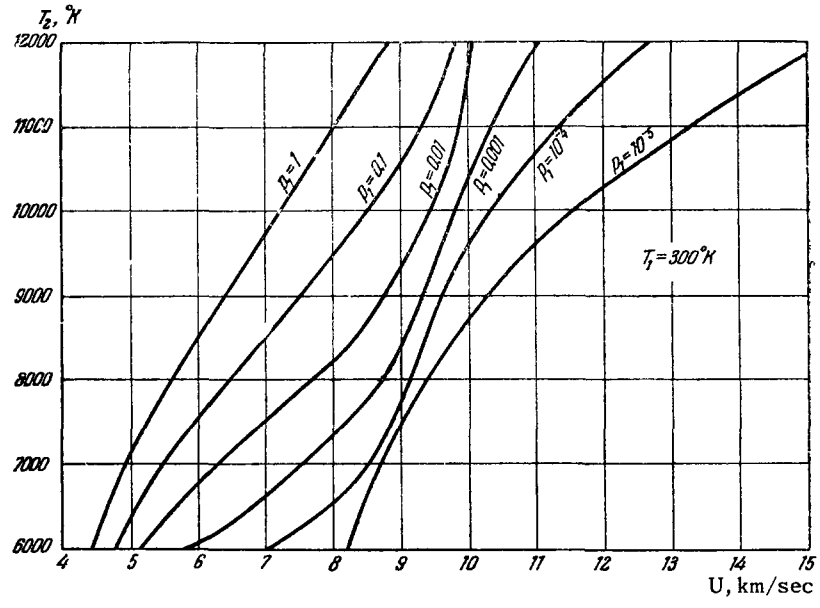

FIG. 4. Temperature behind a plane shock front in air at different initial pressures (in atmospheres) as a function of shock-wave velocity.

$$\frac{\rho}{\rho_0} = \frac{U}{U-u} \quad \text{and} \quad \frac{P}{P_0} = \frac{U}{RT_0} + 1.$$

2. THERMODYNAMIC PROPERTIES OF AIR AND OTHER GASES AT HIGH TEMPERATURES

The thermodynamic equilibrium parameters of a gas behind a shock wave in air and other gases can be calculated using experimentally determined constants. Rozhdestvenskiĭ[9] has performed detailed machine calculation for air up to T = 12,000°K behind a shock wave. Figure 4 shows the shock-velocity dependence of the air temperature behind the shock for different initial pressures ahead of the shock.

Air under the given conditions is a mixture of chemically reacting components (O_2 and N_2 dissociate and NO is generated). The calculations therefore require exact information concerning the equilibrium constants of the reactions as well as the dissociation energies. Interpretation of the nitrogen spectrum leads to two different values for the dissociation energy of the N_2 molecule: 7.38 and 9.76 ev. Many experiments have been performed to determine which value is correct; measurements of detonation velocities in mixtures with C_2N_2 have been in agreement with the value 9.76 ev.[10] The same results have been obtained by Semenov[11] from experiments with flow around models in a shock tube through independent recording of the shock wave velocity and angle of inclination of the associated compression discontinuity at the nose of the model.

The data given in reference 12 also favor the larger value of the dissociation energy, although the experimental procedure unfortunately involves the reflection of a shock wave from a solid wall.

The most convincing answer to the question of the correct nitrogen dissociation energy has been given in references 13 and 14. Here the above described high-explosive method was used to plot shock adiabats of air and other gases, which are shown in Fig. 5; in 1 and 3 the experimental points agree with a calculation using 9.76 ev. The good agreement of the experimental data with calcula-

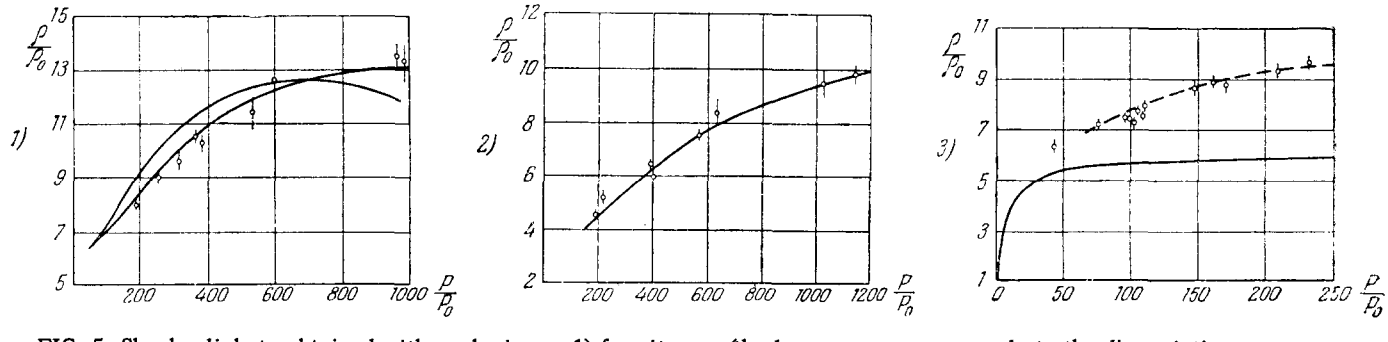

FIG. 5. Shock adiabats obtained with explosives: 1) for nitrogen (the lower curve corresponds to the dissociation energy 9.76 ev); 2) for argon; 3) for air (the continuous curve represents a calculation for an ideal gas; the dashed curve represents a calculation with 9.76 ev nitrogen-dissociation energy).

tions assuming thermodynamic equilibrium behind the shock indicate that equilibrium is reached quite rapidly. Thus for nitrogen at T = 9,000° K equilibrium is reached in less than 10^{-7} sec.[13]

3. SHOCK WAVE PROPAGATION IN A RELAXING GAS

Kantrowitz[15,16] showed experimentally that with the rapid changes of the state of matter it is necessary to take into account in gas dynamics the lag in the excitation of molecular rotational and vibrational degrees of freedom. Zel'dovich[17] and D'yakov[18] performed corresponding theoretical calculations for two-dimensional shock waves.

The possible lag of the energy distribution between molecular degrees of freedom would result in an irreversible energy exchange accompanied by higher entropy and a corresponding change of the gas parameters. Kantrowitz recorded these changes using a total-head (Pitot) tube of small diameter (about 0.1 mm) placed in a steady subsonic gas stream. The gas stopping time, which was determined by means of the flow velocity and tube diameter, amounted to tenths of a microsecond in the case of CO_2. The lag was observed through the change in the difference between the stagnation pressure and the static pressure in the reservoir from which the gas flowed. Using the relation

$$\Delta S(\tau) = R \ln \frac{p_0}{p_{\text{stag}}},$$

where $\Delta S(\tau)$ depends on the specific heats of the different gas-molecular degrees of freedom, the outflow temperature, the tube diameter and the flow velocity, the relaxation time τ can be determined even when it is comparable with the stopping time. The relaxation time obtained in this manner[19] is in good agreement with supersonic data; under normal conditions for the vibrational modes of CO_2 a value of 3 to 6 microseconds is found, depending on moisture content; 1 or 2×10^{-8} sec is obtained for the rotational modes of H_2.

Nonequilibrium relaxation zones behind shocks in such gases as CO_2 and Cl_2 were observed by many investigators,[20-23] who usually photographed the density distribution behind shocks by means of an interferometer, although it was difficult to register zones narrower than 1 mm with this technique.

Narrow zones are observed more conveniently by means of photometry using intense light pulses passing through a Toepler optical system.[24] Figure 6 shows a sketch of this technique and a typical curve representing the density variation behind a shock.

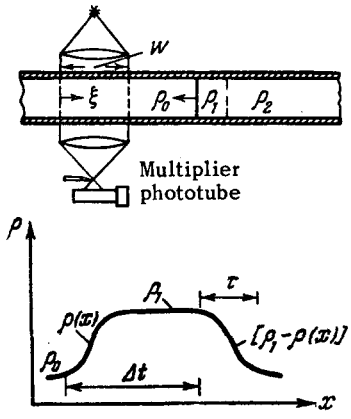

FIG. 6

A slit of width w, parallel to the passing shock front, is located in a tube of rectangular cross section. The intensity of the light passing through the schlieren system with slit width w as a function of the density change in the volume of gas bounded by the slit is given by

$$J(t) = K \int_0^w \frac{\partial \rho(\xi, t)}{\partial \xi} d\xi = K [\rho(w, t) - \rho(0, t)].$$

Thus if the slit is wider than the nonequilibrium zone, the light intensity recorded when the shock wave enters and leaves the field of view bounded by the slit will directly indicate the density distribution behind the shock. If the slit is narrower than the zone, the signal will correspond to the density gradient behind the shock. The sensitivity of this method is about 0.4% of the initial density; the time resolution is limited principally by the requirement of exact adjustment of the optical apparatus and may amount to tenths of a microsecond. The same technique cannot be used with strong waves because of the intrinsic luminosity of the gas behind the shock.

In experiments to determine the relaxation time of CO a time record was obtained of the infrared emission from the gas behind the shock.[25] In these experiments the rise time of the recording unit was of the order of 30 μ sec, which effectively limited the possibility of recording small values of the relaxation time. At an initial pressure of 0.24 atmos the relaxation time of CO was 77 μ sec, corresponding to about 19 μ sec at normal pressure.

For investigating the nonequilibrium zone of the chemical reaction in which a new product is formed, extensive use is being made of optical methods that provide a time record of the absorptivity variation in the gas mixture behind the shock; in a certain portion of the spectrum this depends on the concentration of the new product. We shall now discuss some characteristics of the chemical reactions that occur behind the shock front.

4. INVESTIGATION OF CHEMICAL REACTIONS IN THE GAS BEHIND A SHOCK FRONT

The temperature, pressure, and other parameters of the gas behind a shock front can be determined by means of the gasdynamical equations when the shock velocity is known or can be measured directly. Therefore the extremely rapid adiabatic heating of the gas to a known homogeneous state at a high temperature can be used to investigate the incipience and development of chemical reactions in the given pressure and temperature intervals and during time intervals that are so short that the usual chemical kinetic methods cannot be utilized. Of practical interest, for example, are studies of the kinetics of dissociation and formation of NO behind a shock passing through air at a velocity above 2 km/sec, the dissociation of water vapor and carbon dioxide etc.

The kinetics of chemical reactions in gases are investigated most conveniently by means of shock tubes. Exothermic chemical reactions are studied in order to determine the features of detonation combustion resulting from the different character of the reaction behind a shock front; the kinetics of dissociation, NO production etc. are studied under different conditions.

4.1 Exothermic Chemical Reactions

The propagation of shock waves which are strong enough to initiate an exothermic reaction in a gas mixture results in a self-maintaining explosion — a detonation wave — in the majority of combustible mixtures. The adiabatic heating and combustion at the detonation wave front usually occurs in a very narrow reaction zone a fraction of a millimeter thick adjacent to the front.[26] However in the case of a highly diluted mixture at low initial pressure or generally in a gas with a low chemical reaction rate (such as a mixture of carbon monoxide and oxygen) the ignition region of the gas does not occupy the entire area of the shock front, being localized near the tube wall and following a spiral path during the progressive motion of the detonation wave as a whole (spinning detonation).

The suggestion by Shchelkin[27] and by Zel'dovich[28] that this effect results from a "break" (change of direction) in the shock front has not been fully confirmed by experiments in which the structure of the spinning detonation front was studied.[29,30] The experiments of Voĭtsekhovskiĭ have indicated that the combustion of the mixture in a spinning detonation occurs in a transverse detonation wave following the main shock front.

FIG. 7. Gas luminosity at a spinning detonation front (photographed at an angle of 45° to the tube axis, the wave velocity being compensated by the film movement).

The photograph in Fig. 7 (obtained by Voĭtsekhovskiĭ[31]) represents a series of successive sweeps of the luminosity at the inner surface of a cylindrical tube. Figure 8 gives the configuration of the disturbances at a spinning detonation front. For the transverse wave AB, seen as a bright luminous region in the photograph, the velocity along a circular arc is close to the forward velocity of the detonation wave as a whole. Therefore, in the coordinate system moving with the transverse wave, fresh gas will flow through the front of the main detonation wave AE at an angle of 45°.

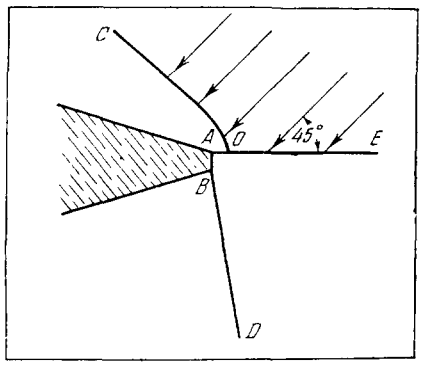

FIG. 8

The combustion products expand behind the transverse wave; this region is shaded in Fig. 8. Fresh gas at the left of the transverse wave flows around the combustion products producing a flow pattern similar to that of supercritical supersonic flow in a corner region (the disconnected compression jump OC).

The perturbation BD, which is inclined at an angle of 12 — 15° to the tube generatrix, is a continuation of the transverse waves and in the form of a luminous line extends for a distance of many tube diameters into the burnt gas region while rotating in phase with the transverse wave. As is shown by the schlieren snapshots of the spinning detonation front in Figs. 9 and 10,[30] spinning deto-

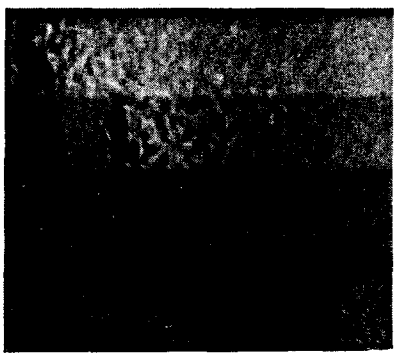

FIG. 9. Schlieren photographs of spinning detonation in a $H_2 + O_2$ mixture, taken at 40,000 frames per second.

FIG. 10. Schlieren snapshot of the gas behind a spinning detonation front in a $H_2 + O_2$ mixture. The wave front is at the extreme left.

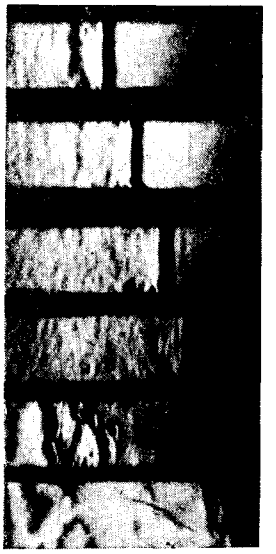

FIG. 11. Successive phases in the ignition of a $H_2 + O_2$ mixture behind a shock wave reflected from a wall, photographed at 35,000 frames per second.

nation is accompanied by strong pressure and density oscillations at a certain frequency in the burnt gas. This means that behind the detonation front running acoustic waves are formed whose circumferential crests are shown by calculations[32] to rotate with a velocity close to that of the detonation, thus producing the extended disturbance trail inclined at a small angle to the tube directrix, which was described above. The velocity of this disturbance along the circumference is thus almost twice the velocity of sound in the burnt gas.

The oscillations of the gas are closely associated with the characteristic slow chemical reaction rate in spinning detonation. The extended reaction zones behind the shock front are unstable and are a cause of the self-oscillating combustion.

The development of ignition in a mixture adiabatically heated by a shock wave has been studied by several authors.[3,33-36] The lag of ignition induced by a shock wave formed at the nose of a projectile was measured and the characteristic oscillatory combustion was observed.[34]

Combustion in a mixture compressed by a shock wave was observed in detail in reference 36. A mixture of hydrogen and oxygen was heated twice — in the incident shock wave and in the wave reflected from the closed tube end. The temperature behind the reflected wave equaled or somewhat exceeded the self-ignition temperature of the mixture, and the heated mixture was at rest with respect to the vessel walls. Schlieren photographs of this process are shown in Fig. 11.

During a certain induction period, which was a function of the mixture pressure and temperature, at several points ignition centers appeared, in which combustion was localized. After this system of centers coalesced, shock discontinuities were formed and detonation ensued.

Under the given experimental conditions the induction period may amount to hundreds of microseconds. At the temperatures and pressures behind the shock front of a detonation wave the induction period may be very much shorter, but even in this case it is of the order of microseconds for many mixtures and must be taken into account in considering the extent of the chemical reaction zone in a detonation wave.

4.2 Investigation of Chemical Reaction Kinetics by Means of Shock Waves

Our knowledge of the kinetics of very fast chemical reactions has been greatly extended by studies employing shock waves. As in the case of earlier methods, experimental techniques were improved in two principal directions: a) by high-speed records of variations in the composition and thermodynamic parameters of mixtures during reactions and b) by halting a reaction after a fixed time interval (the method of "freezing") followed by chemical analysis of the reaction products.

The first part of this classification includes the experiments of Davidson and his coworkers,[37,38] who studied dissociation kinetics behind shock waves in such gases as N_2O_4 and I_2. The time variation of gas composition behind the wave was determined by recording the absorptivity of the separate components in certain portions of their absorption spectra.

The high reaction velocity, the low emissivity and absorptivity of the gas and the luminosity of

easily excited impurities are all factors which lead to the requirement of high resolving power of the optical and electronic equipment for observing the reaction zone in a stream of gas behind a shock wave.

In some instances the course of a reaction is observed by optical means in a gas which is at rest with respect to the vessel walls; this occurs when a shock wave is reflected from a closed tube end. For example, in reference 39 this procedure was used to study thermal dissociation of water vapor from 2400 to 3200° K, and considerable new information was obtained concerning the kinetics of the reaction. The spectroscopic study of the mixture involved photometric examination of the time variation of hydroxyl radical absorptivity at 3064 A.

Great interest attaches to the kinetics of the combining of oxygen and nitrogen, which occurs at 2000 — 3000° K. The basic characteristics of the mechanism and rate of this reaction have been thoroughly studied in a monograph,[40] where the chain character of the reaction was shown on the basis of detonations in various combustible mixtures containing nitrogen as an impurity. In distinction from the bimolecular mechanism for a chain reaction the reaction rate constant must depend on the oxygen concentration through the relationship

$$k_2 = \frac{C}{\sqrt{O_2}},$$

where instantaneous concentration is denoted. This formula was derived experimentally by the authors although their technique had a resolving power of only 10^{-2} sec.

Glick et al.[41] report experiments to determine the reaction rate of nitrogen and oxygen in a shock tube. The mixture was compressed and heated to the required temperature in both the incident and the reflected shock waves. After rapid heating the gas was in the condition required for the reaction, which proceeded for a few tenths of a millisecond, after which it was suddenly cooled by the rarefraction wave, the reacting mixture thus being "frozen." The amount of nitric oxide produced was determined by chemical analysis. The experiment thus determined the time interval Δt from the beginning of the reaction until it was stopped, the instantaneous concentration of nitric oxide after this time and the pressure and temperature of the mixture during the reaction.

The reaction rate is represented by

$$\frac{d\mathrm{NO}}{dt} = k_1 \mathrm{N_2} \cdot \mathrm{O_2} - k_2 \mathrm{NO}^2$$

where k_1 and k_2 are the reaction rate constants of the forward and reverse reactions, with

$$\frac{k_1}{k_2} = \frac{[\mathrm{NO}]^2}{[\mathrm{N_2}]\cdot[\mathrm{O_2}]},$$

where the square brackets denote equilibrium concentrations of the reactants. Under the given experimental conditions the ratio NO/[NO] is always less than 0.3, which by means of the foregoing relations gives an approximate expression for k_2:

$$\frac{d\mathrm{NO}}{dt} \cong k_2 \{[\mathrm{NO}]^2 - \mathrm{NO}^2\}$$

or

$$k_2 \cong \frac{\Delta \mathrm{NO}}{[\mathrm{NO}]^2 \Delta t}.$$

Figure 12 shows the experimental reaction rate constants to be inversely proportional to the square root of the oxygen concentration. This confirms the chain mechanism proposed by Semenov[40] for the given reaction.

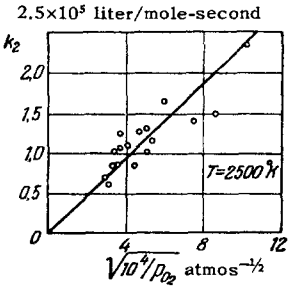

FIG. 12. Dependence of the reaction rate constant on oxygen concentration in the reaction $N_2 + O_2 \underset{k_2}{\overset{k_1}{\rightleftarrows}} 2NO$

It should be noted that this "freezing" technique for studying chemical reaction kinetics possesses certain important practical advantages over the direct optical recording of the course of a reaction. The latter technique requires highly sensitive optical equipment to record a reaction of very short duration in an extended reaction zone.

5. SPECTROSCOPIC INVESTIGATIONS OF THE STATE OF THE GAS BEHIND A SHOCK WAVE

Spectroscopic techniques are very important for studying the state of a high-temperature gas behind a shock wave. Gas spectra excited by shock waves and sweeps of individual spectral regions were studied in references 42 and 43.

To determine the gas temperature behind a shock front, Sobolev and his coworkers[44] developed a number of spectral techniques. Study of the relative intensities of pairs of lines from impurities in the gas[45] yielded less reliable results than a generalized method of line reversal[46] because of the great dependence on shock-tube wall effects and

the influence of impurities on the state of the investigated gas.

The line-reversal technique determines independently the intensity I_X of a gas emission line and the difference between the emission intensity of this line when the gas is transilluminated by a comparison source and the emission intensity of the comparison source itself $(I_{X+S} - I_S)$. The gas temperature is calculated by means of the formula

$$T_x = T_s \left[1 + \frac{\lambda T_s}{C} \ln \left(1 - \frac{I_{x+s} - I_s}{I_x} \right)^{-1} \right].$$

Figure 13 represents temperature measurements behind a shock in nitrogen and air using the generalized method of spectral line reversal in a shock tube with pulse photometry. The solid curve represents the calculation based on thermodynamic equilibrium with 9.76 ev for the dissociation energy of nitrogen. The data indicate that thermodynamic equilibrium is established rapidly in air over a broad range of shock wave velocities and confirm the given choice of nitrogen dissociation energy.

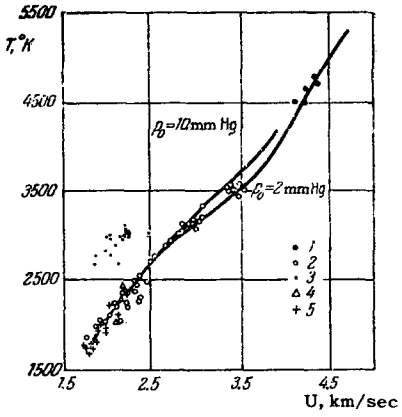

FIG. 13. Temperature behind a shock, measured optically (Sobolev et al.): 1) P_0 = 2 mm Hg, air; 2) P_0 = 10 mm Hg, air; 3) P_0 = 50 mm Hg, air (combustion at the contact surface); 4) P_0 = 10 mm Hg, nitrogen; 5) P_0 = 50 mm Hg, nitrogen.

The spectroscopic study of gases in shock tubes encountered difficulty because of the presence of walls. Behind a shock with M ~ 7 the luminosity of impurities in an entire tube cross section varies with time as shown in Fig. 14. The luminous pulse consists of two signals, the first of which results from the existence of impurities throughout the entire gas volume, while the second increases with the growth of the wall layer and is concentrated in a layer 5 to 7 mm thick at the walls. The wall effect can be eliminated by the use of explosive-induced shock waves, as in the work done by Model'.[47]

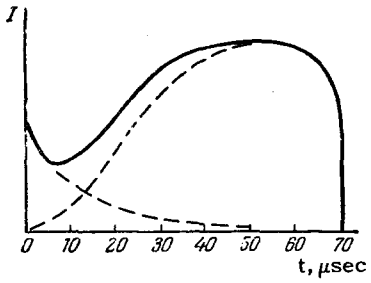

FIG. 14

A continuous spectrum is emitted as the result of thermal ionization behind the shocks and the production of free electrons. With a considerable degree of ionization the lines are shifted and widened by the electric fields of positive ions (the Stark effect). Both phenomena can be used to determine the degree of ionization behind a shock.[42]

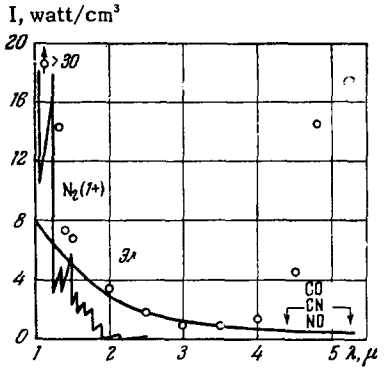

FIG. 15. Infrared spectrum of air at a high temperature behind a shock.

A shock-tube study of the continuous infrared spectrum of air yielded the data given in Fig. 15.[48] The long-wave emission above two microns cannot be accounted for by the molecular spectrum of nitrogen (the first solid curve in Fig. 15). Calculations show that this emission results from the collisions of free electrons with nitrogen and oxygen atoms; the potential of this interaction was determined in reference 49. The second solid curve in Fig. 15 was plotted with this potential taken into account, corresponding to an elastic scattering cross section of 10^{-15} cm^2 for oxygen atoms.

6. THERMODYNAMIC EQUILIBRIUM IN GAS IONIZATION BEHIND A SHOCK WAVE

The measurement of the electrical conductivity of thermally ionized air behind a shock[50] has shown that for shock waves with M ~ 15 thermodynamic equilibrium is attained very rapidly. The experimental technique is shown schematically in Fig. 16. The tube in which the shock wave propagates is

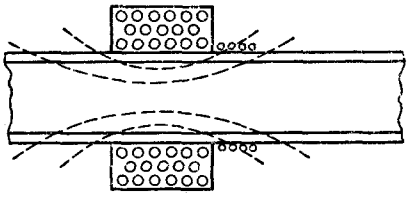

FIG. 16. Schematic diagram of experiment to measure the electrical conductivity of a gas behind a shock.

surrounded by a current-bearing coil. The varying magnetic field in the conducting gas induces an emf in a second coil placed next to the first coil; the electrical conductivity of the gas is thereby determined. This apparatus was calibrated by propelling metal bars differing in conduction through the tube.

In investigations of argon and other inert gases for M = 10 to 18, which corresponds to degrees of ionization up to 25%, it has been observed that a fairly considerable time is required for the establishment of thermodynamic equilibrium (tens of microseconds).[51,52] This was studied in detail by the authors of reference 51, who determined experimentally the distribution of the electrostatic potential, induced by electron diffusion, in the gas behind the shock front, and also measured the lag of the continuous gas spectrum excited only by electron-ion recombination at some distance from the shock front.

Of the most probable ionization mechanisms — such as electron-atom collisions or collisions between atoms and photoionization — the electron-collision mechanism is the most efficient. However, at the initial instant of time, when the electron density is zero, the initial degree of ionization must be produced by another mechanism. The electron-collision mechanism begins to function after this preliminary phase is concluded. The electrons suffer large energy losses since the ionization potential of argon is 15.7 ev and kT for an electron is about 1 ev. The energy of the electron gas is replenished through elastic collisions of "cold" electrons with atoms and ions.

Because of the large difference between the masses of atoms and electrons the energy exchange is a slow process and determines the time required to establish thermodynamic equilibrium in the gas. Figure 17 shows the ionization lag of argon, observed in reference 51, as a function of the temperature behind a shock and of M. The solid line represents the theoretical calculation of the authors.

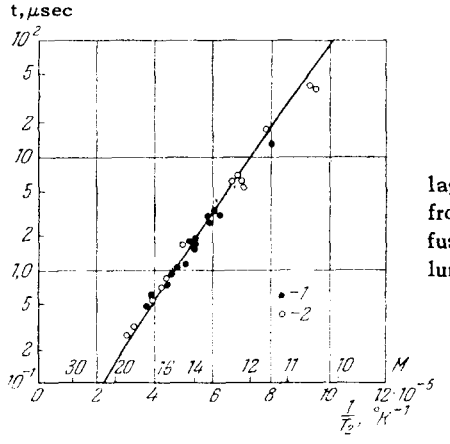

FIG. 17. Ionization lag behind a shock front in argon: 1) diffusion potential; 2) luminosity lag.

[1] Ya. B. Zel'dovich and Yu. P. Raĭzer, Usp. Fiz. Nauk **63**, 613 (1957).

[2] W. Payman and W. C. F. Shepherd, Proc. Roy. Soc. (London) **A186**, 293 (1946).

[3] T. V. Bazhenova and R. I. Soloukhin, Seventh International Symposium on Combustion, London, 1958, BJ-613.

[4] S. G. Zaĭtsev, Приборы и техника эксперимента (Instruments and Measurement Engineering) No. 6 (1958).

[5] Resler, Lin, and Kantrowitz, J. Appl. Phys. **23**, 1390 (1952), Russ. Transl. in symposium Механика (Mechanics) No. 5 (1953).

[6] H. Mark, J. Aeronaut. Sci. **24**, 304 (1957).

[7] R. Strehlow and A. Cohen, J. Chem. Phys. **28**, 983 (1958).

[8] R. H. Christian and F. L. Yarger, J. Chem. Phys. **23**, 2042 (1955).

[9] I. B. Rozhdestvenskiĭ, Symp. Физихеская газодинамика (Physical Gasdynamics), U.S.S.R. Acad. Sci., 1959; V. V. Selivanov and I. Ya. Shlyapintokh, J. Phys. Chem. (U.S.S.R.) No. 3 (1958).

[10] Kistiakowsky, Knight, and Malin, J. Chem. Phys. **20**, 876 (1952).

[11] S. S. Semenov, Dokl. Akad. Nauk SSSR **114**, 841 (1957).

[12] J. P. Toennies and E. F. Greene, J. Chem. Phys. **23**, 1366 (1955).

[13] Christian, Duff, and Yarger, J. Chem. Phys. **23**, 2045 (1955).

[14] W. E. Deal, J. Appl. Phys. **28**, 782 (1957).

[15] A. Kantrowitz, J. Chem. Phys. **14**, 150 (1946).

[16] P. W. Huber and A. Kantrowitz, J. Chem. Phys. **15**, 275 (1947).

[17] Ya. B. Zel'dovich, J. Exptl. Theoret. Phys. (U.S.S.R.) **16**, 365 (1946).

[18] S. P. D'yakov, J. Exptl. Theoret. Phys. (U.S.S.R.) **27**, 728 (1954).

[19] W. Griffith, J. Appl. Phys. **21**, 1319 (1950).

[20] W. Griffith, Phys. Rev. **87**, 234 (1952).

[21] Smiley, Winkler, and Slawsky, J. Chem. Phys. **20**, 923 (1952).

[22] E. F. Smiley and E. H. Winkler, J. Chem. Phys. **22**, 2018 (1954).

[23] Griffith, Brickle, and Blackman, Phys. Rev. **102**, 1209 (1956).

[24] E. L. Resler and M. Scheibe, J. Acoust. Soc. Am. **27**, 932 (1955).

[25] Windsor, Davidson, and Taylor, J. Chem. Phys. **27**, 315 (1957).

[26] Ya. B. Zel'dovich and A. S. Kompaneets, Теория

детонации (Theory of Detonations), U.S.S.R. Acad. Sci. 1955.

[27] K. I. Shchelkin, Dokl. Akad. Nauk SSSR **47**, 482 (1945).

[28] Ya. B. Zel'dovich, Dokl. Akad. Nauk SSSR **52**, 147 (1946).

[29] B. V. Voĭtsekhovskiĭ, Dokl. Akad. Nauk SSSR **114**, 717 (1957).

[30] R. I. Soloukhin, Труды IV конф. ЭНИН (Trans. IV Conf. of Inst. of Power Engineering), Acad. Sci. U.S.S.R., Moscow, 1957.

[31] B. V. Voĭtsekhovskiĭ, Труды МФТИ (Trans. Moscow Physico-Technical Inst.), Phys. Ser. Moscow, 1958.

[32] J. A. Fay, J. Chem. Phys. **20**, 942 (1952).

[33] Gershanik, Zel'dovich, and Rozlovskiĭ, J. Phys. Chem. (U.S.S.R.) **24**, 85 (1950).

[34] Ya. B. Zel'dovich and I. Ya. Shlyapintokh, Dokl. Akad. Nauk SSSR **65**, 871 (1949).

[35] Berets, Greene, and Kistiakowsky, J. Am. Chem. Soc. **72**, 1086 (1950).

[36] S. G. Zaĭtsev and R. I. Soloukhin, Dokl. Akad. Nauk SSSR **122**, 1039 (1958).

[37] T. Carrington and N. Davidson, J. Phys. Chem. **57**, 418 (1953).

[38] Britton, Davidson, and Schott, Disc. Faraday Soc. **17**, 58 (1954).

[39] Bauer, Schott, and Duff, J. Chem. Phys. **28**, 1089 (1958).

[40] Zel'dovich, Sadovnikov, and Frank-Kamenetskiĭ, Окисление азота при горении (Oxidation of Nitrogen in Combustion), U.S.S.R. Acad. Sci., 1947.

[41] Glick, Klein, and Squire, J. Chem. Phys. **27**, 850 (1957).

[42] Petschek, Rose, Glick, Kane, and Kantrowitz, J. Appl. Phys. **26**, 83 (1955).

[43] A. R. Fairbairn and A. G. Gaydon, Proc. Roy. Soc. (London) **A239**, 464 (1957).

[44] Sobolev, Potapov, Kitaeva, Faĭzullov, Aliamovskiĭ, Antropov, and Isaev, Izv. Akad. Nauk SSSR, Ser. Fiz. **22**, 730 (1958), Columbia Tech. Transl. p. 725.

[45] N. N. Sobolev, Тр. Физ. ин-та АН СССР (Trans. Phys. Inst. Acad. Sci. U.S.S.R.) **7**, 159 (1956).

[46] A. G. Sviridov and N. N. Sobolev, J. Exptl. Theoret. Phys. (U.S.S.R.) **24**, 93 (1953).

[47] I. Sh. Model', J. Exptl. Theoret. Phys. (U.S.S.R.) **32**, 714 (1957), Soviet Phys. JETP **5**, 589 (1957).

[48] Wentink, Planet, Hammerling, and Kivel, J. Appl. Phys. **29**, 742 (1958).

[49] Hammerling, Shine, and Kivel, J. Appl. Phys. **28**, 760 (1957).

[50] L. Lamb and S. C. Lin, J. Appl. Phys. **28**, 754 (1957). Russ. Transl. in Symp. Вопросы ракетн. техн. (Problems of Rocket Technology) No. 3, 1958.

[51] H. Petschek and S. Byron, Annals of Physics **1**, 270 (1957).

[52] W. Roth and P. Gloersen, J. Chem. Phys. **29**, 820 (1958).

Translated by I. Emin